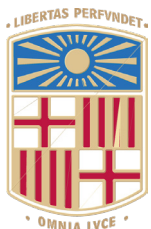


Book of Tutorials and Abstracts



European Microbeam Analysis Society

EMAS 2025

18th
EUROPEAN WORKSHOP

on

MODERN DEVELOPMENTS AND APPLICATIONS IN MICROBEAM ANALYSIS

11 to 15 May 2025
at the
TecnoCampus
Mataró (Barcelona), Spain

Organized in collaboration with the
Universitat de Barcelona, Spain

EMAS

European Microbeam Analysis Society eV

www.microbeamanalysis.eu/

This volume is published by:

European Microbeam Analysis Society eV (EMAS)

EMAS Secretariat

c/o Eidgenössische Technische Hochschule, Institut für Geochemie und Petrologie

Clausiusstrasse 25

8092 Zürich

Switzerland

© 2025 *EMAS* and authors

ISBN 978 90 8227 6985

NUR code: 972 – Materials Science

All rights reserved. No part of this publication may be reproduced, stored in a retrieval system, or transmitted in any form or by any means, electronic, mechanical, by photocopying, recording or otherwise, without the prior written permission of *EMAS* and the authors of the individual contributions.



**COMBINING NANO-CT AND ELECTRON MICROSCOPY FOR SCALE-BRIDGING
3D ANALYSIS OF NANOPARTICULATE AND POROUS FUNCTIONAL
MATERIALS**

Erdmann Spiecker

Friedrich-Alexander-Universität Erlangen-Nürnberg, Institute of Micro- and Nanostructure Research (IMN) & Center for Nanoanalysis and Electron Microscopy (CENEM),
Cauerstrasse 3, 91058 Erlangen, Germany
e-mail: erdmann.spiecker@fau.de

Erdmann Spiecker is Full Professor and Head of the Institute of Micro- and Nanostructure Research (IMN) in the Department of Materials Science at the University of Erlangen-Nürnberg (Germany). He also serves as the spokesperson for the Center for Nanoanalysis and Electron Microscopy (CENEM), which integrates state-of-the-art instrumentation, expertise, and methodological innovation for advanced materials microscopy at the university.

Professor Spiecker's research focuses on the development and application of high-resolution, analytical, and tomographic electron microscopy techniques to investigate the structure, chemistry, and structure-property relationships of a broad range of materials. These include thin films and heterostructures, 2D materials, nanoparticles, organic solar cells, catalytic systems, and high-temperature materials. His work emphasises the close integration of methodological advancements in microscopy with their application in materials research.

A particular emphasis of his research lies in *in situ* microscopy, which provides direct insight into dynamic processes at the microscopic scale. In this area, he served as the spokesperson for the DFG Research Training Group 1896 "In *situ* microscopy with electrons, X-rays, and scanning probes," which supported early-career researchers through a collaborative and interdisciplinary research environment. Another key focus of Professor Spiecker's work is scale-bridging 3D characterisation of materials using complementary tomographic techniques. In addition to electron tomography, he actively explores X-ray microscopy and nano-computed tomography (nano-CT) to systematically extend 3D characterisation capabilities to larger length scales.

1. ABSTRACT

Functional materials often comprise particles and pores, with structural characteristics spanning various length scales that together govern their overall properties. A comprehensive characterisation of the 3D structure of such materials, therefore, requires the combination of different tomography techniques, which together cover the corresponding length scales in terms of addressable sample volumes, achievable resolution and the required information content (e.g., structure, chemical composition). In this contribution, we present methods and research work developed and carried out at the Center for Nanoanalysis and Electron Microscopy (CENEM) in Erlangen with the particular aim of bridging the gap between the nano- and microscale in the 3D analysis of materials.

Figure 1 shows an overview of the key tomography techniques that enable 3D analysis of materials at the micro- and nanoscale. It also indicates the range of sample sizes each method can accommodate, along with their corresponding spatial resolutions. Electron tomography (ET), nano-CT and micro-CT are non-destructive tomography methods for which preparation is generally required, but the analysed volume remains intact during the analysis. In contrast, atom probe tomography (APT) and focussed ion beam (FIB) tomography – also known as 3D-FIB or slice & view – are destructive, i.e., the analysed sample volume is consumed during the examination. For the non-destructive tomography methods, the achievable spatial resolution generally decreases with increasing sample volume. This is different with the 3D-FIB method, where the examined sample volume and the achievable resolution are in principle decoupled, provided that no preparation artefacts dominate.

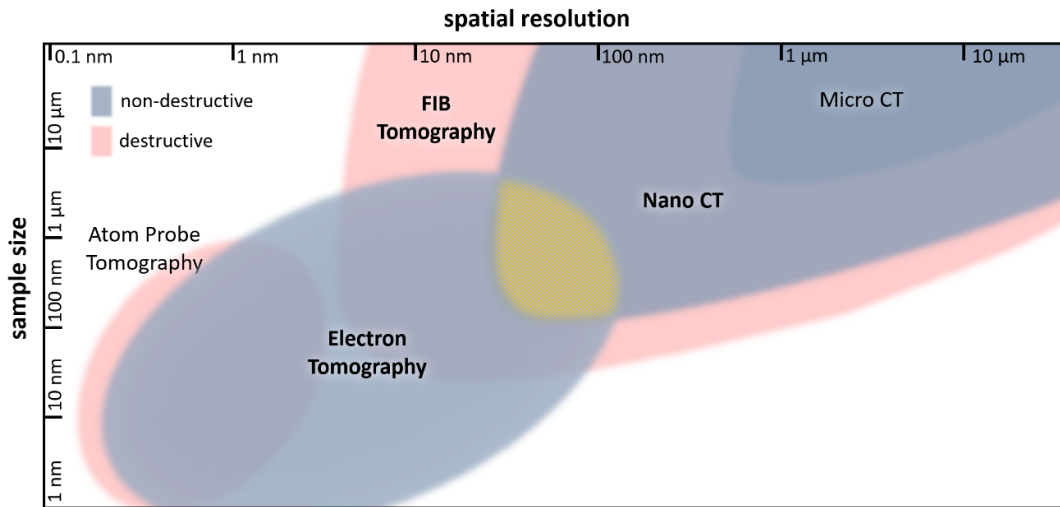


Figure 1. High-resolution tomography techniques for 3D characterisation of materials (adopted from C. Kübel). The dashed area indicates the overlap of electron tomography and lab-based nano-CT in terms of accessible sample size and spatial resolution.

One particularly interesting field is the overlap between ET and nano-CT (Fig. 1, shaded area), which has the potential to combine two non-destructive methods for bridging the gap between nano- and microscale in the cross-scale 3D analysis of materials. This combination has great potential, especially for functional materials with hierarchical structures, such as those found in the complex electrodes of Li-ion batteries or electrolyzers. The combination and correlation of these two methods has received relatively little attention to date, as laboratory-based nano-CT devices have only become more widespread in recent years and the two methods are typically used in different communities. As shown in Fig. 1, 3D-FIB ideally covers the transitional range between the nano- and microscale and can therefore serve as a valuable complementary technique – provided its destructive nature is not a limiting factor.

In electron tomography (ET), a distinction is made between conventional and 360°-ET, whereby the latter is sometimes also referred to as on-axis or full-range ET (Fig. 2a). In conventional ET, the sample can only be analysed in a limited tilt angle range of typically $\pm 70^\circ$, as the sample itself or the sample holder causes shadowing at higher tilt angles. In addition, the projected sample thickness of typical TEM samples with slab geometry increases significantly at high tilt angles, which reduces the quality of these projections. Due to the limited tilt angle range, so-called missing-wedge artefacts occur in the 3D reconstruction, which can only be corrected for under certain assumptions [1]. In contrast, 360°-ET enables images to be taken in the complete tilt angle range so that missing-wedge artefacts can be excluded. For this, however, the sample must be prepared free-standing on a tip and be electron transparent in all projections. This can be realised for a bulk material by pillar preparation using FIB cutting or for particulate systems by transferring individual particles to the tomography tip. For the latter, we have developed a ‘stamping transfer’ method that works in the SEM and reliably enables the transfer of selected particles from a lacey C-grid to the tip (Fig. 2b) [2]. For nanoparticles, natural adhesion is usually sufficient for the transfer process; for particles in the micrometre range, SEM adhesive may have to be used to transfer the particle to the tip. The ‘stamping transfer’ method has been developed for 360° CT but can also be used for nano-CT.

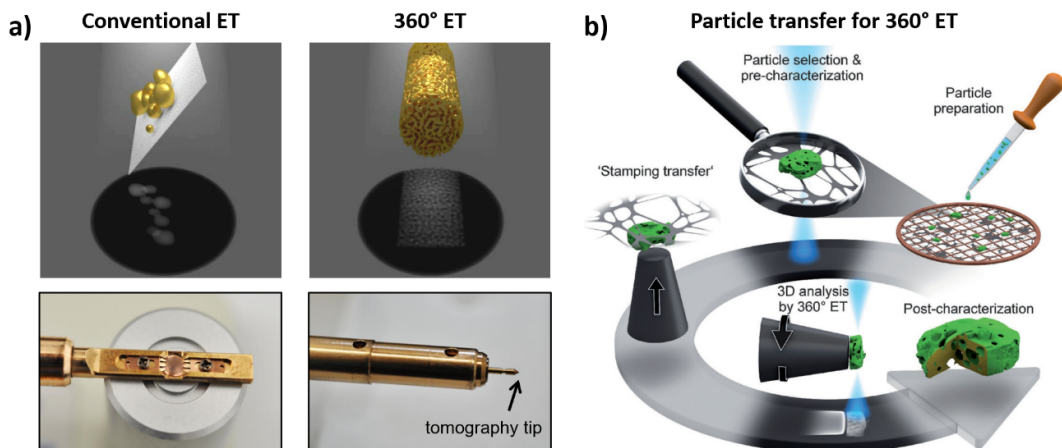


Figure 2. a) Conventional versus 360° electron tomography; b) ‘Stamping transfer’ technique enabling preparation of nano and microparticle for 360° ET and nano-CT [2].

Figure 3 shows examples of successful ‘stamping transfer’ of particles of different sizes onto a tomography tip: a) A micro/macro-porous zeolite particle with dimensions in the range of several micrometres, b) A colloidal supraparticle, consisting of 190 nm primary polystyrene (PS) spheres, with total diameter of $\sim 4 \mu\text{m}$, and c) An approx. 70 nm hematite nanoparticle with enclosed pores. Detailed 3D analyses of these particles using 360°-ET can be found in Ref. [3], Figs. 4a to 4c), and Ref. [2], respectively. The ‘stamping transfer’ method can, therefore, be used over a wide range of particle sizes from the nm range to the μm range. An alternative method for the preparation of particles for 360°-ET was introduced by Padgett *et al.* [4]. Here, weakly absorbing carbon nanofibres are attached to the tomography tip and serve as a carrier for the nanoparticles, which adhere to the nanofibres. With this preparation method, the particles are not completely free-standing, but several particles can be analysed at the same time.

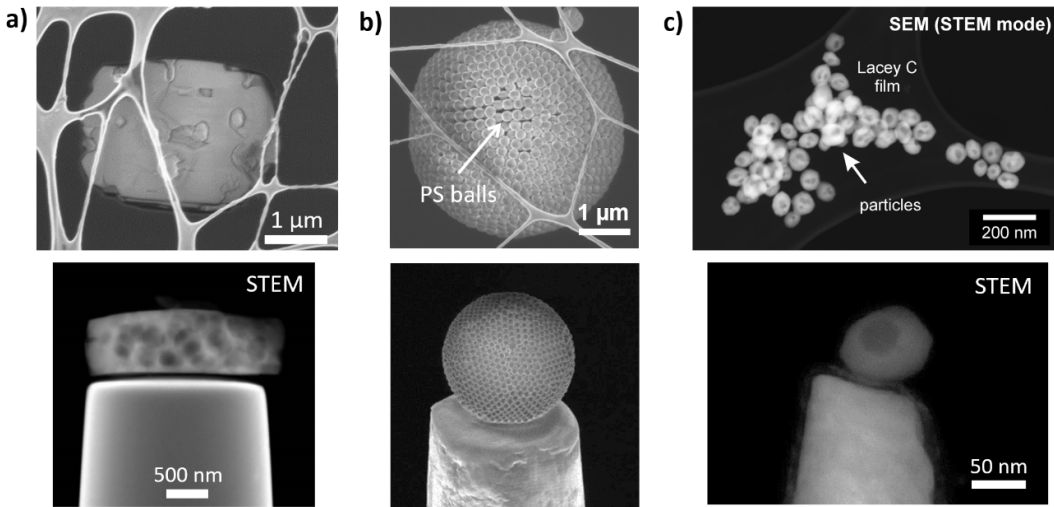


Figure 3. Examples of successful “stamping transfer” onto tomography tips for 360° ET and nano-CT: a) Micro/macro-porous zeolite particle, b) Colloidal photonic supraparticle, c) Porous hematite nanoparticle [2, 3, 5, 6].

As an example of 3D analysis, Figs. 4a and 4b presents the results of 360°-ET of the supraparticle shown in Fig. 3b. The surface rendering in Fig. 4a reveals that the supraparticle is crystalline and exhibits icosahedral symmetry [5]. However, the cross-section through the tomogram shown in Fig. 4b clearly reveals disordered regions within the particle (highlighted in red), characterised by a lower packing density of the primary PS particles. This observation aligns well with the molecular dynamics simulation shown in Fig. 4c, which predicts such disordered regions as a consequence of the self-assembly process during supraparticle formation.

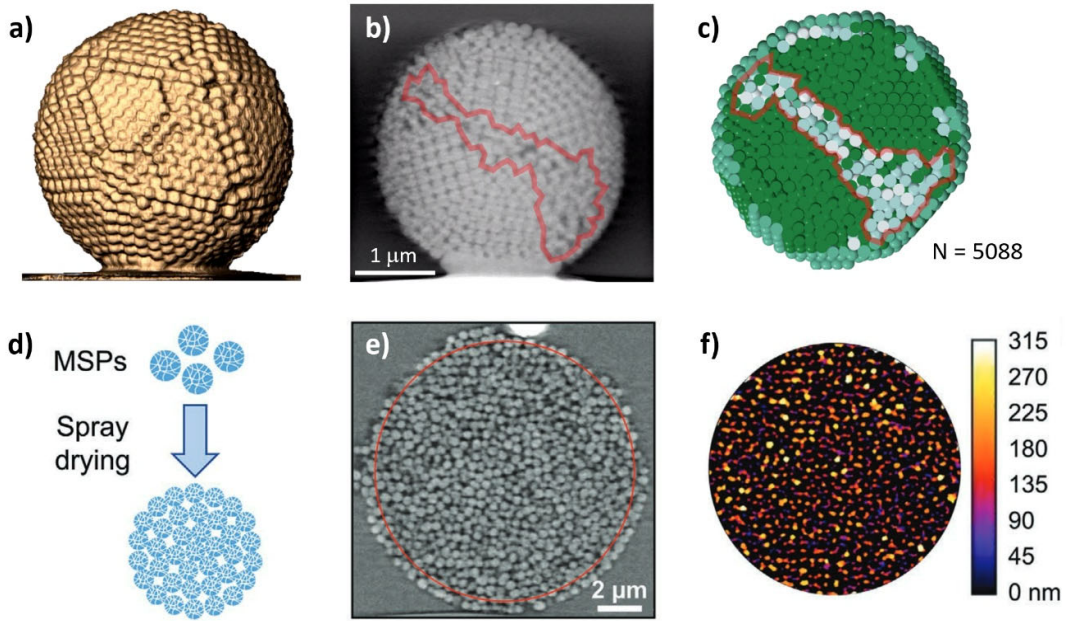


Figure 4. a to c) 360°-ET of colloidal supraparticle prepared by stamping transfer (Fig. 3b) reveals disordered regions in the icosahedral particle structure, in good agreement with atomistic simulations [5]; d to f) Nano-CT analysis of a spray-dried supraparticle with hierarchical porosity. The particle is composed of mesoporous silica particles (MSPs) and additionally reveal mostly macroporous interparticle pore space, analysed in f) [8].

The supraparticle shown in Figs. 4a and 4b has a diameter of approximately 4 μm , which approaches the upper size limit for ET analysis. Nevertheless, the results demonstrate that 360°-ET based on annular dark-field (ADF) scanning transmission electron microscopy (STEM) imaging was still capable of revealing the internal structure of the supraparticle, including the positions of most of the primary PS particles. However, if the size of the supraparticle becomes significantly larger, ET is no longer feasible. Fortunately, nanoCT is a non-destructive tomography method that can take over in this size range (Fig. 1). Alternatively, 3D FIB can also be used [7], although the method is destructive and, depending on the material, special measures must be taken to avoid curtaining and melting of the primary particles during cutting. Figures 4d to 4f shows an example of a nano-CT analysis of a significantly larger supraparticle with a diameter of approx. 13 μm , which was fabricated by spray-drying of mesoporous silica primary particles. The aim of the study was to synthesise a hierarchical pore structure for applications in catalysis and chromatography by combining the intrinsic mesopores (a few nanometres in size) of the primary silica particles with the predominantly macropores ($> 50 \text{ nm}$) formed by interparticle voids within the supraparticle. The cross-section through the nano-CT tomogram in Fig. 4e demonstrates that nano-CT is well-suited for tomographic analysis at this scale, meeting both sample size and resolution requirements. By applying the maximum sphere inscription method, the local macropore sizes can be visualized (Fig. 4f) and further analysed to determine the average pore size distribution [8].

Figure 5a shows the components and a simplified beam path of the Zeiss Xradia 810 Ultra X-ray microscope/nano-CT used in this study. The most important components are the Fresnel zone plate, which serves as the objective lens, and the phase ring, which is located in the back focal plane of the objective lens and generates Zernike phase contrast. In order to address different sample sizes, the microscope provides two magnification modes: a large field-of-view (LFOV) mode with an image field of $65 \mu\text{m} \times 65 \mu\text{m}$ and an optical resolution of 150 nm and a high-resolution (HRES) mode with an image field of $16 \mu\text{m} \times 16 \mu\text{m}$ and an optical resolution of slightly better than 50 nm (Fig. 5b). For samples composed of light elements, X-ray attenuation at an energy of 5.4 keV (Cr-K α) is too low to achieve sufficient absorption contrast for the sample sizes under consideration. Phase contrast offers advantages here, as significantly higher contrasts are achieved. At the same time, however, phase contrast cannot be interpreted using the classic Lambert-Beer law, which makes evaluation more difficult and leads to well-known artefacts ('halo' and 'shade off'). However, since most functional materials consist primarily of relatively lighter elements, there is no alternative to using phase contrast in many cases.

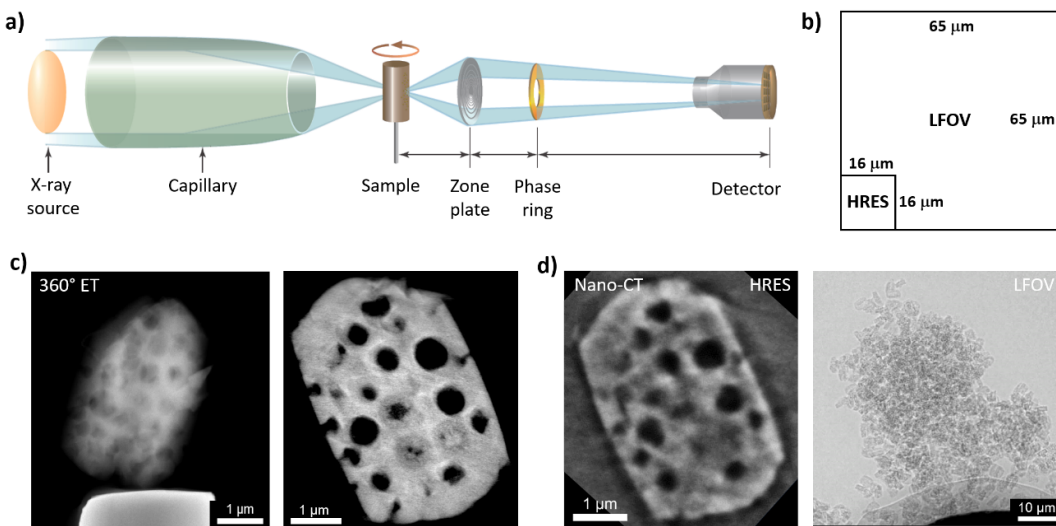


Figure 5. a) Components and schematic ray path of the lab-based X-ray microscope/nano-CT Zeiss Xradia 810 Ultra (adopted from Zeiss company). b) Field of views (FOV) of the high-resolution (HRES) and the large field of view (LFOV) modes. The corresponding optical resolutions are ~ 150 nm and ~ 50 nm, respectively. c and d) Correlative 360°-ET and nano-CT of identical macroporous zeolite particle. While 360°-ET provides slightly better resolution, nano-CT enables investigation of thousands of particles when using the LFOV mode (adopted from [3]).

Figures 5c and 5d show an example of a direct correlation between 360°-ET and nano-CT, performed on a micro/macroporous zeolite particle that was transferred to a tomography tip using the stamping-transfer method. For comparison, identical sections through the tomograms

obtained by 360°-ET and nano-CT are shown side by side. It is clearly evident that, despite the large sample size, 360°-ET still provides noticeably higher spatial resolution. In contrast, nano-CT – particularly in LFOV mode – not only enables the study of one individual particle but also allows imaging and analysis of agglomerates consisting of hundreds of particles (Fig. 5d, right). Further details on this study can be found in Ref. [3].

As a final example, a multi-scale 3D characterisation workflow is introduced, combining micro-CT, nano-CT, and analytical FIB-SEM-EDXS (Fig. 6). This approach enables comprehensive analysis across a wide range of length scales and is specifically suited for particle composite materials with particles ranging from 0.3 μm to 15 μm in size. A key challenge lies in distinguishing mixtures of particle systems with varying chemical compositions, especially when the particles exhibit similar size and density. The study focuses on a synthetic mixture of minerals – calcite, talc, dolomite, and magnesite – that share comparable morphology, size distribution, and elemental composition. The analysis begins with micro-CT to assess particle morphology and spatial distribution within a larger, consolidated volume. This is followed by nano-CT imaging of a smaller, site-specifically ablated pillar sample, allowing for higher-resolution investigations with direct Z-contrast, enabled by the use of a quasi-monochromatic X-ray beam (Fig. 6b). To further enhance material differentiation, the nano-CT reconstruction is correlated with SEM-BSE imaging and energy-dispersive X-ray spectrometry (EDS) mapping performed on FIB cross-sections (Fig. 6c). This integrated approach allows for the identification and classification of particles based on their distinct chemical signatures. The quality and depth of the analysis are further improved through advanced post-processing and multidimensional data analysis techniques, enabling a quantitative evaluation of particle size distribution, phase composition, and the degree of mineral liberation – defined as the accessibility of individual particle components.

2. ACKNOWLEDGEMENTS

The author thanks the members of the Erlangen tomography group for their contributions, in particular Benjamin Apeleo-Zubiri, Thomas Przybilla, Silvan Englisch, Allison Götz, and Janis Wirth. He further thanks the collaboration partners from the research groups of Nicolas Vogel (FAU Erlangen), Michael Engel (FAU Erlangen), Wilhelm Schwieger (FAU Erlangen), Urs Peuker (TUBA Freiberg) and Volker Schmidt (University Ulm). Financial support by the German Research Foundation (DFG) through the project SP648/8 “High-resolution X-ray microscopy for correlative tomography, high throughput screening and in situ mechanical testing of structural and functional materials” (Project-ID 316992193), the research training group GRK1896 “In situ Microscopy with Electrons, X-rays and Scanning Probes” (Project-ID: 218975129), and the Collaborative Research Centre 1411 “Design of Particulate Products” (Project-ID 416229255) is highly appreciated.

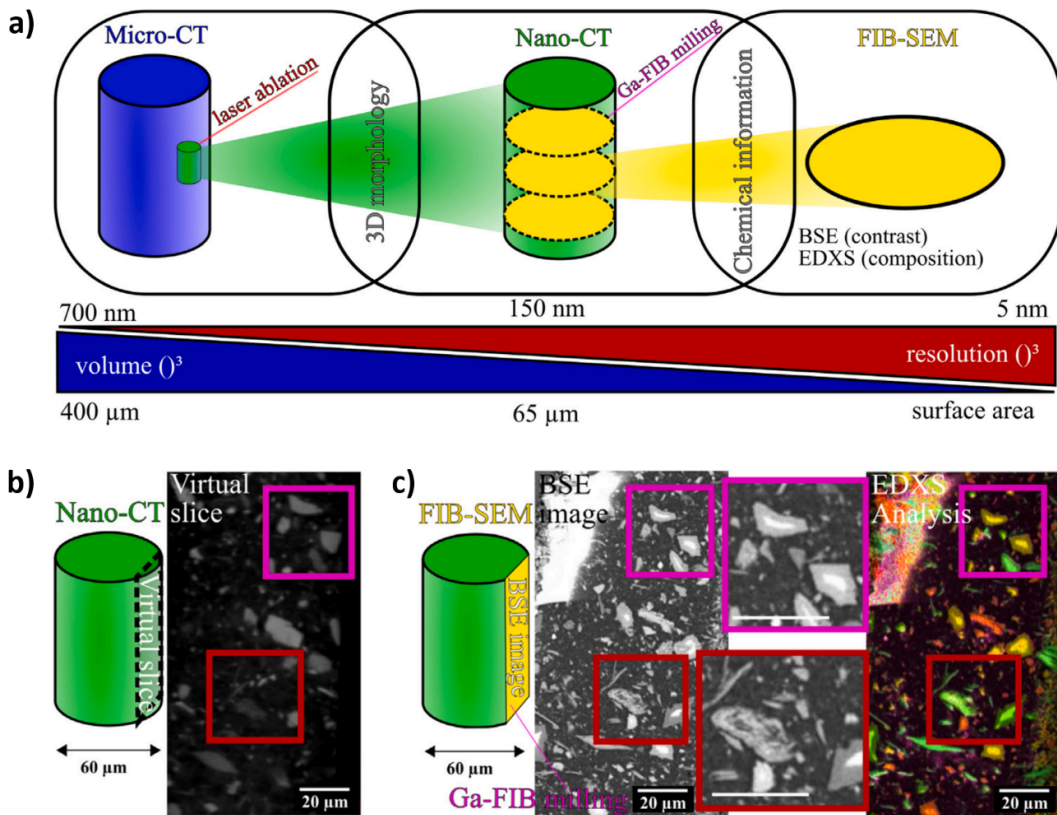


Figure 6. a) Workflow combining micro-CT, nano-CT and analytical FIB-SEM for classification of mineral microparticles in particle mixtures. b and c) illustrates the correlation of nano-CT and FIB-SEM-EDXS: b) Virtual slice through nano-CT tomogram, c) BES image (left) and composed EDS map (right) of sample area corresponding to the virtual slice, providing training data for segmentation and labelling of particles and mineral phases in the nano-CT data. Chemical information from SEM-EDS is essential for reliable discrimination of the mineral phases [9].

3. REFERENCES

- [1] Goris B, Van den Broek W, Batenburg K J, Heidari Mezerji H and Bals S 2012 *Ultramicroscopy* **113** 120-130
- [2] Przybilla T, Zubiri B A, Beltrán A M, Butz B, Machoke A G F, Inayat A, Distaso M, Peukert W, Schwieger W and Spiecker E 2018 *Electron Tomography* **2** 1700276
- [3] Apeleo Zubiri B, Wirth J, Drobek D, Englisch S, Przybilla T, Weissenberger T, Schwieger W and Spiecker E 2021 *Adv. Mater. Interfaces* **8** 2001154
- [4] Padgett E, Hovden R, DaSilva J C, Levin B D A, Grazul J L, Hanrath T and Muller D A 2017 *Microsc. Microanal.* **23** 1150-1158
- [5] Wang J, Mbah C F, Przybilla T, Englisch S, Spiecker E, Engel M and Vogel N 2019 *ACS Nano* **13** 9005-9015

- [6] Distaso M, Apeleo Zubiri B, Mohtasebi A, Inayat A, Dudák M, Kočí P, Butz B, Klupp Taylor R, Schwieger W, Spiecker E and Peukert W 2017 *Microporous Mesoporous Mater.* **246** 207-214
- [7] Wang J, Liu Y, Bleyer G, Goerlitzer E S A, Englisch S, Przybilla T, Mbah C F, Engel M, Spiecker E, Imaz I, Maspoch D and Vogel N 2022 *Angewandte Chemie – Int. Ed.* **61** e202117455
- [8] Sultan U, Götz A, Schlumberger C, Drobek D, Bleyer G, Walter T, Löwer E, Peuker U A, Thommes M, Spiecker E, Apeleo Zubiri B, Inayat A and Vogel 2023 *Small* **19** 2300241
- [9] Englisch S, Ditscherlein R, Kirstein T, Hansen L, Furat O, Drobek D, Leißner T, Apeleo Zubiri B, Weber A P, Schmidt V, Peuker U A and Spiecker E 2023 *Powder Technol.* **419** 118343

